Volume 23, No 3 | International Journal of Radiation Research, July 2025

Application value of amide proton transfer combined with relative cerebral blood volume in grading adult diffuse glioma and predicting isocitrate dehydrogenase gene mutation status

S. Chen[1], R. Huang[1*], J. Chen[1], H. Lin[1], L. Lu[2], S. Zhang[1], Z. Jiang[3]

[1]*Department of Radiology, Quanzhou First Hospital, Quanzhou, Fujian, China*
[2]*Department of Radiotherapy, Quanzhou First Hospital, Quanzhou, Fujian, China*
[3]*Department of Neurosurgery, Quanzhou First Hospital, Quanzhou, Fujian, China*

► ***Original article***

Corresponding author:
Risheng Huang, M.D.,
E-mail: *hrisheng@126.com*

Received: July 2024
Final revised: October 2024
Accepted: November 2024

Int. J. Radiat. Res., July 2025; 23(3): 737-742

DOI: 10.61186/ijrr.23.3.31

Keywords: *Glioma, grade, isocitrate dehydrogenase, gene.*

ABSTRACT

Background: This research attempted to elucidate amide proton transfer (APT) role in combination with relative cerebral blood volume (rCBV) in grading adult diffuse glioma and predicting isocitrate dehydrogenase (IDH) gene mutation status. ***Materials and Methods:*** A retrospective analysis was implemented on 70 patients with adult diffuse glioma in our hospital from September 2022 to October 2023. All patients underwent Dynamic Susceptibility Contrast Perfusion Weighted Imaging (DSC-PWI) and APT-weighted magnetic resonance imaging examination. The values of rCBVmax and APTmean in differentiating the classification of glioma and IDH gene mutation status were analyzed. ***Results:*** The rCBVmax and APTmean value were reduced in grade II patients than in grade III patients (P<0.01). The AUC of rCBVmax value combined with APTmean value was 0.9330, with a 95% CI of 0.8962-0.9697, which was higher than single rCBVmax value or APTmean value (P<0.001). The rCBVmax value and APTmean were higher in IDH wild-type glioma patients than in IDH mutant-type glioma patients (P<0.01). The AUC of rCBVmax value combined with APTmean value was 0.8808, with a 95% CI of 0.8233-0.9383, which was higher than single rCBVmax value or APTmean value (P<0.001). ***Conclusion:*** The combined diagnosis of APT and rCBV can improve the value of differentiating grade I and II glioma as well as IDH genotyping, which is worth of promoting in clinical practice.

INTRODUCTION

Glioma is the most common primary intracranial malignancy. Pathological biopsy is gold standard for diagnosis of glioma [1]. Because gliomas contain different histological features, there may be errors based on traditional histopathological diagnostic sampling, resulting in under grading and even false negative results [2]. In addition, there are differences in diagnosis caused by pathologists' subjective knowledge based only on tumor cell and morphological classification [3]. With the publication of the 2016 and 2021 editions of the *WHO Classification of Central Nervous System Tumors*, the classification of gliomas has evolved from histology to one in which histological, biological and molecular characteristics jointly define tumor types [4].

Isocitrate dehydrogenase (IDH) is the vital driving gene of diffuse glioma [5]. Mutations in isocitrate dehydrogenase exists in 70-80% of stage II and III astrocytomas, oligodendrogliomas, and most secondary glioma, accounting for about 10% of all GBM [6]. In contrast, IDH mutations are almost never found in primary glioma [7]. In malignant gliomas, mutated IDH proteins are almost universally expressed in tumor cells, and IDH mutations precede secondary and tertiary genetic lesions, suggesting that IDH mutations are an early etiological event in the development of glioma subsets [8].

Magnetic resonance imaging (MRI) is major imaging method to evaluate the grade of adult diffuse glioma before clinical surgery [9]. Dynamic Susceptibility Contrast Perfusion Weighted Imaging (DSC-PWI) is currently the mainstream method for evaluating glioma grading [10]. In classification of cerebral glioma, relative cerebral blood volume (rCBV) is a reliable parameter for evaluating the grade of glioma. The increase of rCBV is associated with microangiogenesis and increased tumor blood supply, and the glioma grade with high rCBV value tends to be higher [11]. However, DSC-PWI is still insufficient in evaluating grade specificity of gliomas, and low rCBV can also be seen in some high-grade glioma [12]. Amide proton transfer (APT)-weighted magnetic resonance imaging is a molecular imaging technique based on the principle of chemical shift saturation exchange [13]. The APT signal reflects concentration of protons in the amide group (-NH) of mobile proteins and polypeptides [14]. In glioma, increased APT signal strength is thought to originate from excess cytoplasm and elevated amide proton concentration in proliferating glioma cells [15]. It has been found that with the increase of APT signal strength, the grade of glioma also increased [16].

[DOI: 10.61882/ijrr.23.3.31]

Though application prospect of APT is promising, there are still some shortcomings. There is currently evidence that APT combined with rCBV can significantly improve diagnostic performance in differentiating recurrent glioma from treatment-related effects [17]. Thus, it is reasonable to believe that APT provides additional information for rCBV in glioma grading and may improve diagnostic accuracy in challenging situations.

In this study, by comparing the imaging data of non-IDH mutation status, the imaging characteristics of IDH mutation types were summarized to improve the reliability of MRI evaluation of glioma IDH genotype, which may provide more valuable information for clinical diagnosis, treatment, and prognosis of brain glioma. This research was the first time to combine APT with rCBV in improving grading accuracy of adult diffuse glioma, so as to carry out early intervention and treatment, with a certain degree of foresight.

MATERIALS AND METHODS

A retrospective analysis received conduction on 70 adult diffuse glioma patients confirmed by postoperative pathology in our hospital from September 2022 to October 2023, among which were 38 males and 32 females, aged 16-64 years, with a median age of 43 years. Among them, there were 40 cases of astroglioma and 30 cases of oligodendroglioma. There were 48 cases of grade II and 22 cases of grade III. According to the World Health Organization (WHO) classification criteria for brain tumors in 2016, 60 patients were diagnosed with IDH wild-type glioma and 10 with IDH mutant-type glioma. This research received authorization by the Ethics Committee of Quanzhou First Hospital [approval No. K053 (2023)].

Inclusion criteria: (1) Clinical symptoms/imaging suggested the possibility of intracranial space occupation, glioma patients could not be clearly excluded; (2) No treatment had been performed; (3) No contraindications for MRI examination. Exclusion criteria: (1) Combined with systemic diseases and other malignant tumors (2) Patients refused to sign informed consent; (3) Patients with a history of massive cerebral infarction, alcoholism, drug abuse, chronic pain and other factors affecting brain structure and metabolism. (4) Pathological findings do not support the diagnosis of glioma in patients.

Dynamic susceptibility contrast perfusion weighted imaging examination

The DSC-PWI sequence adopted gradient-recalled echo-planar (GRE-EPI) sequence. Each patient was scanned in 20 layers, each layer was scanned in 60 phases, a total of 1200 images were scanned, and the imaging time was 1 minute and 36 seconds. When the scan reached phase 4, the exogenous contrast agent gadobenate dimeglumine (Gd-BOPTA; MultiHance®, Bracco, Milano, Italy) was injected with a double-barrel high-pressure syringe and a 19G trocar inserted through the median cubital vein. The dosage was 0.1-0.2 mmol/kg, the injection rate was 5 ml/s, and the injection time was less than 5 s. After the injection of contrast agent, 20 ml normal saline was injected immediately. Scanning parameters: Time of repeatation (TR) = 1500 ms, Time of Echo (TE) = 30 ms, turning angle = 90°, Field of Vision (FOV) = 220 mm × 220 mm, matrix = 128×128, layer thickness = 5 mm, layer spacing=1 mm.

Amide proton transfer examination

Axial phase acquisition of T1-weighted imaging (T1WI): TR/TE: 2034/20 ms, layer thickness = 5 mm, FOV =230×210 mm, matrix was 328×258, scanning time was 1 minute 54 seconds.

Axial phase acquisition of T2-weighted imaging (T2WI): TR/TE=3000/105 ms, layer thickness was 5 mm, FOV: 230 × 210 mm, matrix: 328×258, scanning time was 1 minute 12 seconds.

Coronal phase acquisition of T2WI-fluid-attenuated inversion-recovery sequency (T2WI-FLAIR): TR/TE: 9000/81 ms, layer thickness: 5 mm, inversion time: 2500 ms, FOV: 230 × 210 mm, matrix: 328×258, scanning time: 1 minute 48 seconds.

Axial phase acquisition of T1WI enhanced scanning: TR/TE: 6.8/3.1 ms, layer thickness: 1 mm, FOV: 240 × 240 mm, matrix: 240 × 240, the scanning time was 3 minutes and 02 seconds, the contrast agent was 10% gabentate meglumine (Gd-DTPA, Omniscan, GE Healthcare, Dublin, Ireland), and the dose was 0.1 mmol/kg body weight. The patient was injected rapidly through the cubital vein with a high pressure syringe at a rate of 3.5 L/s, and then rinsed with normal saline at an equal volume and rate.

Axial phase plane acquisition of diffusion weighted imaging (DWI) image: B values of DWI were selected as B=1000 and B=0 s/mm^2, TR /TE: 3741/80 ms, layer thickness: 5 mm, FOV: 230×210 mm, FOV: phase 100%, matrix: 128 × 97, the scan time was 2 minutes 59 seconds. The apparent diffusion coefficients (ADCs) of the regions of interest for B=0 and B=1000 were collected, respectively.

Axial phase acquisition of APT-weighted imaging: TR/TE: 6306/8.3 ms, layer thickness: 5 mm, FOV: 230×180 mm, matrix: 128×100, scanning time was 3 minutes and 42 seconds.

Image post-processing

All original DSC-PWI images were processed by Perfusion MR Software and Mean Curve software. Firstly, a region of interest (ROI) received placing in middle layer on phase where signal intensity of original image changed the most, and the artery inflow function (AIF) diagram was drawn. T2* signal intensity-time curve arterial inflow function (AIF)

[DOI: 10.61882/ijrr.23.3.31]

diagram referred to the signal-time curve of normal arteries in the layer. The time range of the first passage of contrast agent was set on the diagram of arterial inflow effect. The range of the left vertical line and the middle vertical line was the baseline, the middle vertical line was the starting point of contrast agent inflow into the artery, and the right vertical line was the end point of contrast agent outflow. The negative curve between the middle vertical line and the right vertical line reflected the change of signals around microvessels. The cerebral blood volume (CBV) pseudo-color map was reconstructed using AIF diagram. By a doctor with 13 years of neuroimaging experience, 5 non-overlapping circular ROIs were placed on the tumor solid enhancement region on the CBV map, and the maximum value was taken as the maximum CBV (CBV_{max}) within the tumor solid region. The ROI size was about 15-20 voxels, 0.1-0.2 cm^2, and the ROI was placed in the tumor solid enhancement area to avoid the bleeding, necrosis, cystic degeneration and large blood vessel area of the tumor as far as possible. Another 5 ROIs were placed in the peritumoral edema area, and the maximum value was taken as the CBV_{max} value in the peritumoral edema area. In addition, 5 ROIs were placed in contralateral normal white matter area of lesion, 5 CBV values were measured, and the average CBV_{CNWM} was taken. If the tumor was located in the midline, the ROI was placed in the right normal white matter area of the lesion. Relative to CBV_{max} ($rCBV_{max}$) = CBV_{max}/CBV_{CNWM}.

The MRI APT data was imported to construct the pseudo-color map, and 5 areas of interest (ROI) were randomly selected in the tumor core area to avoid the tumor vascular and cystic necrosis areas. The same number of areas of interest was checked in the normal white matter area of the tumor on the opposite side for control. The maximum value (APT_{max}), minimum value (APT_{min}) and mean value of APT intensity in the tumor core were recorded [APT_{mean}, (APT1+APT2+APT3+APT4+APT5) ÷5].

Operative tissue specimens received re-evaluation with the newest 2016 WHO classification of central nervous system tumors by an experienced pathologist in a blinded manner. The IDH gene mutation status received assessment through specific polymerase chain reaction.

Statistical analysis

SPSS 24.0 statistical software (IBM Corp., Armonk, NY) was adopted for data analysis. Measurement data received representation as (x±s), with t-test adopted for comparisons. Count data received representation as (n, %), with χ^2 test adopted for comparisons. The diagnostic efficacy of parameters received analysis with receiver operating characteristic curve (ROC) to distinguish grade I and II gliomas. P<0.05 meant statistical significance.

RESULTS

Cerebral blood volume value of the solid part of glioma

The pathological assay depicted that $rCBV_{max}$ value demonstrated a marked decline in grade II patients in comparison to that in grade III patients (P<0.01, figure 1).

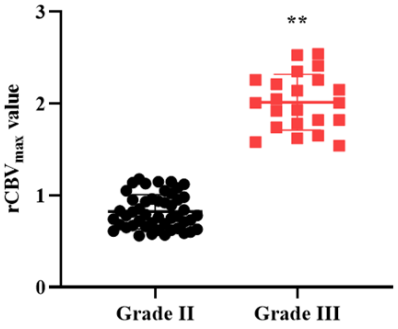

Figure 1. rCBVmax value of solid part of glioma in different pathological grades. **P<0.01.

Amide proton transfer value of the solid part of glioma

The pathological assay depicted that APT_{mean} value demonstrated a marked decrease in grade II patients in comparison to that in grade III patients (P<0.01, figure 2).

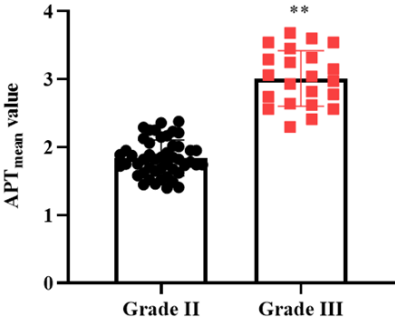

Figure 2. APTmean value of solid part of glioma in different pathological grades. **P<0.01.

Value of $rCBV_{max}$ and APT_{mean} in differentiating grade I and II gliomas

ROC curve indicated that the AUC of $rCBV_{max}$ value was 0.7951, with a 95% CI of 0.7230-0.8672, the AUC of APT_{mean} value was 0.8022, with a 95% CI of 0.7291 -0.8754, and the AUC of $rCBV_{max}$ value combined with APT_{mean} value was 0.9330, with a 95% CI of 0.8962-0.9697, which depicted elevation in comparison to single $rCBV_{max}$ value or APT_{mean} value (P<0.001, figure 3).

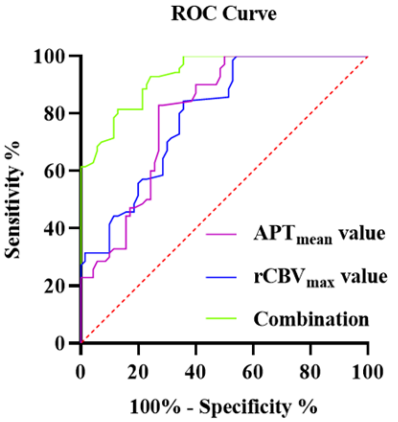

Figure 3. Value of rCBVmax value and APTmean value in differentiating grade I and II gliomas.

[DOI: 10.61882/ijrr.23.3.31]

$rCBV_{max}$ value of the solid part of glioma in different groups

The $rCBV_{max}$ value depicted a remarkable elevation in IDH wild-type glioma patients in comparison to that in IDH mutant-type glioma patients (P<0.01, figure 4).

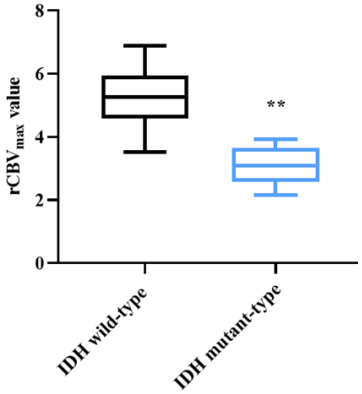

Figure 4. rCBVmax value of the solid part of glioma in different groups. **P<0.01.

APT_{mean} value of the solid part of glioma in different groups

The APT_{mean} value depicted a remarkable elevation in IDH wild-type glioma patients in comparison to that in IDH mutant-type glioma patients (P<0.01, figure 5).

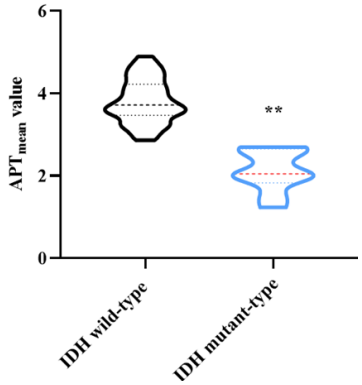

Figure 5. APTmean value of the solid part of glioma in different groups. **P<0.01.

Value of $rCBV_{max}$ and APT_{mean} in differentiating isocitrate dehydrogenase wild- and mutant-type gliomas

ROC curve indicated that the AUC of $rCBV_{max}$ value was 0.8055, with a 95% CI of 0.7336-0.8774, the AUC of APT_{mean} value was 0.8027, with a 95% CI of 0.7292 -0.8761, and the AUC of $rCBV_{max}$ value combined with APT_{mean} value was 0.8808, with a 95% CI of 0.8233-0.9383, which depicted elevation in comparison to single $rCBV_{max}$ value or APT_{mean} value (P<0.001, figure 6).

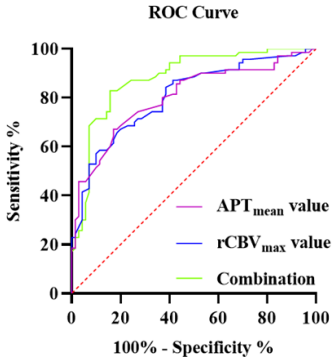

Figure 5. APTmean value of the solid part of glioma in different groups. **P<0.01.

DISCUSSION

MRI has the advantages of high tissue resolution, multi-parameter and multi-sequence imaging, and is a common imaging method for the diagnosis of glioma [18]. Conventional MRI can observe tissue bleeding, tumor parenchymal necrosis, and surrounding white matter edema with high diagnostic sensitivity, but the observed enhancement is caused by contrast agent overflow caused by the destruction of the blood barrier, and it is difficult to differentiate grade II and III glioma [19]. With the progression of glioma, a large number of new blood vessels are formed, which can provide nutrients for the proliferation of tumor cells [20]. The development of microvessels shows the following trends: (1) High permeability, but no abnormal perfusion; (2) Perfusion is higher, but permeability is not abnormal; (3) Permeability and perfusion were abnormal [21]. Therefore, single perfusion technique cannot comprehensively evaluate the blood perfusion of cerebral glioma microvessels.

Herein, we applied APT combined with rCBV to explore the grading accuracy of adult diffuse glioma, and the results indicated that the $rCBV_{max}$ value and APT_{mean} value were lower in grade II patients than in grade III patients and the AUC of $rCBV_{max}$ value combined with APT_{mean} value was higher than single $rCBV_{max}$ value or APT_{mean} value, suggesting that the combined diagnosis of APT and rCBV could improve the value of differentiating grade II and III glioma. Because rCBV is significantly correlated with endothelial growth factor and tumor vascular density, the rCBV value in the region with high microvascular density is higher than that in the region with low density, so the rCBV value in grade III glioma is higher than that in grade II [22], which depicts consistency with our findings. APT imaging can produce contrast, which is largely dependent on the concentration of endogenous cellular proteins in the tissue and the exchange properties of amide protons with water molecules (depending on pH), while other parameters, such as tissue water content, water T1 value and saturation efficiency, also affect contrast [23]. Our findings further validated clinical value of combined diagnosis of APT and rCBV in gliomas.

IDH1 and IDH2 mutation states belong to genetic markers that define the top of an emerging molecular classification scheme located in different glioma subpopulations [24]. IDH status offers outstanding utility as an objective biomarker that complements existing histology and provides an accurate diagnosis. In adult-type diffuse glioma, IDH evaluation is required for all types [25]. Relative to IDH wild-type glioma, patients with IDH mutant glioma have a much better prognosis [26]. A large meta-analysis depicted that IDH mutants existed relation to longer overall survival, regardless of classification [27]. Preliminary genomic studies of IDH mutation status in WHO2/3 grade glioma have shown that patients with IDH

[DOI: 10.61882/ijrr.23.3.31]

mutations present different molecular characteristics in comparison with patients with IDH wild-type [28]. Mutant IDH acquired a new enzymatic activity to convert alpha-ketogluta rate (α-KG) to 2-hydroxyglutarate (2-HG), which resulted in higher production of 2-HG in glioma cells [29]. 2-HG activates α-KG dependent prolyl hydroxylase, which promotes hypoxia-inducible factors-1α (HIF-1α) degradation and inhibits aggressive tumor behaviors (such as angiogenesis) [30]. Doll *et al*. applied quantitative proteomics to study the changes of signal transduction pathways and protein expression in IDH1 mutant brain glioma cells, and the results showed that the whole histone expression was down-regulated in IDH1 mutant tumor cells [31]. A series of microscopic changes caused by IDH mutation provide a theoretical basis for MRI evaluation and prediction of IDH mutation status [32]. Currently, there are few studies on the correlation between APT and molecular typing of brain glioma, and there is still room to further explore the relationship between different APT imaging characteristics and tumor molecular changes. Herein, $rCBV_{max}$ value and APT_{mean} value were higher in IDH wild-type glioma patients than in IDH mutant-type glioma patients, and AUC of $rCBV_{max}$ value combined with APT_{mean} value was higher than single $rCBV_{max}$ value or APT_{mean} value, suggesting that combined diagnosis of APT and rCBV could improve value of IDH genotyping, which was in accordance with previous studies [33, 34].

Certain limitations also existed in this research. Our research sample size was small. Moreover, this research depicts a retrospective characterization. Furthermore, data may exist possibility of measurement bias.

CONCLUSION

Our research innovatively clarify that combined diagnosis of APT and rCBV can improve the value of differentiating grade Ⅱ and Ⅲ glioma as well as IDH genotyping, which is worth of promoting in clinical practice.

ACKNOWLEDGMENT

None.

Funding: This work was supported by the Natural Science Foundation of Fujian Province, China (No. 2023J011772).

Conflicts of interests: The authors declared no conflict of interest.

Ethical consideration: All patients signed a documented, voluntarily informed consent form. All methods were carried out in compliance with the Helsinki Declaration criteria, and this study was authorized by the Ethics Committee of Quanzhou First Hospital with the approval No. K053 (2023).

Author contribution: S.C.; conceived and designed experiments. R.H., J.C., and H.L.; contributed markedly to experiments and arranging data. L.L., Z.J.; conducted data analysis. S.Z.; wrote draft manuscript. S.C., R.H.; revised manuscript. All authors read and approved final manuscript.

REFERENCES

1. Miller AM, Shah RH, Pentsova EI, Pourmaleki M, Briggs S, Distefano N, *et al.* (2019) Tracking tumour evolution in glioma through liquid biopsies of cerebrospinal fluid. *Nature,* ***565****(7741): 654-8*.
2. Azad TD and Bettegowda C (2022) Longitudinal monitoring of diffuse midline glioma using liquid biopsy. *Neuro-oncology,* ***24****(8): 1375-6*.
3. Gusyatiner O and Hegi ME (2018) Glioma epigenetics: From subclassification to novel treatment options. *Seminars in Cancer Biology,* ***51****: 50-8*.
4. Horbinski C, Berger T, Packer RJ, Wen PY (2022) Clinical implications of the 2021 edition of the WHO classification of central nervous system tumours. *Nature Reviews Neurology,* ***18****(9): 515-29*.
5. Mellinghoff IK, Ellingson BM, Touat M, Maher E, De La Fuente MI, Holdhoff M, *et al.* (2020) Ivosidenib in isocitrate dehydrogenase 1-mutated advanced glioma. *Journal of Clinical Oncology,* ***38****(29): 3398-406*.
6. Yan X, Ji H, Liu Z, Ma S, Dong J, Jiang X, *et al.* (2022) Characterization of the ferroptosis-related genes for prognosis and immune infiltration in low-grade glioma. *Frontiers in Genetics,* ***13****: 880864*.
7. Eckel-Passow JE, Lachance DH, Molinaro AM, Walsh KM, Decker PA, Sicotte H, *et al.* (2015) Glioma groups based on 1p/19q, IDH, and TERT promoter mutations in tumors. *The New England Journal of Medicine,* ***372****(26): 2499-508*.
8. Dang L, Jin S, Su SM (2010) IDH mutations in glioma and acute myeloid leukemia. *Trends in Molecular Medicine,* ***16****(9): 387-97*.
9. Li G, Li L, Li Y, Qian Z, Wu F, He Y, *et al.* (2022) An MRI radiomics approach to predict survival and tumour-infiltrating macrophages in gliomas. *Brain,* ***145****(3): 1151-61*.
10. Song S, Wang L, Yang H, Shan Y, Cheng Y, Xu L, *et al.* (2021) Static (18)F-FET PET and DSC-PWI based on hybrid PET/MR for the prediction of gliomas defined by IDH and 1p/19q status. *European Radiology,* ***31****(6): 4087-96*.
11. Kickingereder P, Wiestler B, Burth S, Wick A, Nowosielski M, Heiland S, *et al.* (2015) Relative cerebral blood volume is a potential predictive imaging biomarker of bevacizumab efficacy in recurrent glioblastoma. *Neuro-Oncology,* ***17****(8): 1139-47*.
12. Schmainda KM, Prah M, Connelly J, Rand SD, Hoffman RG, Mueller W, *et al.* (2014) Dynamic-susceptibility contrast agent MRI measures of relative cerebral blood volume predict response to bevacizumab in recurrent high-grade glioma. *Neuro-Oncology,* ***16*** *(6): 880-8*.
13. Milot L (2022) Amide proton transfer-weighted MRI: Insight into cancer cell biology. *Radiology,* ***305****(1): 135-6*.
14. Lee DW, Heo H, Woo DC, Kim JK, Lee DH (2021) Amide proton transfer-weighted 7-T MRI contrast of myelination after cuprizone administration. *Radiology,* ***299****(2): 428-34*.
15. Jiang S, Eberhart CG, Zhang Y, Heo HY, Wen Z, Blair L, *et al.* (2017) Amide proton transfer-weighted magnetic resonance image-guided stereotactic biopsy in patients with newly diagnosed gliomas. *European Journal of Cancer,* ***83****: 9-18*.
16. Wu M, Jiang T, Guo M, Duan Y, Zhuo Z, Weng J, *et al.* (2023) Amide proton transfer-weighted imaging and derived radiomics in the classification of adult-type diffuse gliomas. *European Radiology,* ***34*** *(5): 2986-2996*.
17. Tang PLY, Méndez Romero A, Jaspers JPM, Warnert EAH (2022) The potential of advanced MR techniques for precision radiotherapy of glioblastoma. *Magma (New York, NY),* ***35****(1): 127-43*.
18. Mandonnet E (2011) Mathematical modeling of glioma on MRI. *Revue Neurologique,* ***167****(10): 715-20*.
19. Bahrami N, Hartman SJ, Chang YH, Delfanti R, White NS, Karunamuni R, *et al.* (2018) Molecular classification of patients with grade II/III glioma using quantitative MRI characteristics. *Journal of Neuro-oncology,* ***139****(3): 633-42*.

[DOI: 10.61882/ijrr.23.3.31]

20. Colquhoun A (2017) Cell biology-metabolic crosstalk in glioma. *Int J Biochem Cell Biol,* ***89****: 171-81.*
21. Liang W, Guo B, Ye J, Liu H, Deng W, Lin C, *et al.* (2019) Vasorin stimulates malignant progression and angiogenesis in glioma. *Cancer Science,* ***110****(8): 2558-72.*
22. Fuss M, Wenz F, Scholdei R, Essig M, Debus J, Knopp MV, *et al.* (2000) Radiation-induced regional cerebral blood volume (rCBV) changes in normal brain and low-grade astrocytomas: quantification and time and dose-dependent occurrence. *Int J Radiat Oncol Biol Phys,* ***48****(1): 53-8.*
23. Chen K, Jiang XW, Deng LJ, She HL (2022) Differentiation between glioma recurrence and treatment effects using amide proton transfer imaging: A mini-Bayesian bivariate meta-analysis. *Frontiers in Oncology,* ***12****: 852076.*
24. Han S, Liu Y, Cai SJ, Qian M, Ding J, Larion M, *et al.* (2020) IDH mutation in glioma: molecular mechanisms and potential therapeutic targets. *Br J Can,* ***122****(11): 1580-9.*
25. Turkalp Z, Karamchandani J, Das S (2014) IDH mutation in glioma: new insights and promises for the future. *JAMA Neurology,* ***71****(10): 1319-25.*
26. Vuong HG, Altibi AMA, Duong UNP, Ngo HTT, Pham TQ, Chan AK, *et al.* (2017) TERT promoter mutation and its interaction with IDH mutations in glioma: Combined TERT promoter and IDH mutations stratifies lower-grade glioma into distinct survival subgroups-A meta-analysis of aggregate data. *Crit Rev Oncol Hematol,* ***120****: 1-9.*
27. Molenaar RJ and Wilmink JW (2022) IDH1/2 Mutations in Cancer stem cells and their implications for differentiation therapy. *J Histochem Cytochem,* ***70****(1): 83-97.*
28. Berger TR, Wen PY, Lang-Orsini M, Chukwueke UN (2022) World Health Organization 2021 Classification of central nervous system tumors and implications for therapy for adult-type gliomas: A review. *JAMA Oncology,* ***8****(10): 1493-501.*
29. Miller JJ (2022) Targeting IDH-mutant glioma. *Neurotherapeutics,* ***19****(6): 1724-32.*
30. Dang L, Yen K, Attar EC (2016) IDH mutations in cancer and progress toward development of targeted therapeutics. *Annals of Oncology,* ***27****(4): 599-608.*
31. Doll S, Urisman A, Oses-Prieto JA, Arnott D, Burlingame AL (2017) Quantitative proteomics reveals fundamental regulatory differences in oncogenic HRAS and isocitrate dehydrogenase (IDH1) driven astrocytoma. *Molecular & cellular Proteomics,* ***16****(1): 39-56.*
32. Roux A, Roca P, Edjlali M, Sato K, Zanello M, Dezamis E, *et al.* (2019) MRI atlas of IDH wild-type supratentorial glioblastoma: probabilistic maps of phenotype, management, and outcomes. *Radiology,* ***293****(3): 633-43.*
33. Álvarez-Torres MDM, Balaña C, Fuster-García E, Puig J, García-Gómez JM (2023) Unlocking bevacizumab's potential: rCBV(max) as a Predictive biomarker for enhanced survival in glioblastoma IDH-wildtype patients. *Cancers,* ***16****(1): 161.*
34. Joo B, Han K, Ahn SS, Choi YS, Chang JH, Kang SG, *et al.* (2019) Amide proton transfer imaging might predict survival and IDH mutation status in high-grade glioma. *European Radiology,* ***29****(12): 6643-52.*

[DOI: 10.61882/ijrr.23.3.31]